Observation of the $D_1(2420) \to D\pi^+\pi^-$ Decays

K. Abe,[7] K. Abe,[40] I. Adachi,[7] H. Aihara,[42] M. Akatsu,[20] D. Anipko,[1] Y. Asano,[45] T. Aushev,[11] T. Aziz,[38] S. Bahinipati,[4] A. M. Bakich,[37] S. Banerjee,[38] I. Bedny,[1] U. Bitenc,[12] I. Bizjak,[12] S. Blyth,[24] A. Bondar,[1] A. Bozek,[25] M. Bračko,[7,18,12] J. Brodzicka,[25] P. Chang,[24] Y. Chao,[24] A. Chen,[22] K.-F. Chen,[24] W. T. Chen,[22] B. G. Cheon,[3] R. Chistov,[11] S.-K. Choi,[5] Y. Choi,[36] A. Chuvikov,[32] J. Dalseno,[19] M. Danilov,[11] M. Dash,[46] A. Drutskoy,[4] S. Eidelman,[1] V. Eiges,[11] F. Fang,[6] S. Fratina,[12] N. Gabyshev,[1] A. Garmash,[32] T. Gershon,[7] G. Gokhroo,[38] B. Golob,[17,12] J. Haba,[7] N. C. Hastings,[7] K. Hayasaka,[20] H. Hayashii,[21] M. Hazumi,[7] T. Higuchi,[7] L. Hinz,[16] T. Hokuue,[20] Y. Hoshi,[40] S. Hou,[22] W.-S. Hou,[24] T. Iijima,[20] A. Imoto,[21] K. Inami,[20] A. Ishikawa,[7] R. Itoh,[7] Y. Iwasaki,[7] J. H. Kang,[47] J. S. Kang,[14] P. Kapusta,[25] S. U. Kataoka,[21] N. Katayama,[7] H. Kawai,[2] T. Kawasaki,[27] H. Kichimi,[7] H. J. Kim,[15] J. H. Kim,[36] S. K. Kim,[35] S. M. Kim,[36] K. Kinoshita,[4] P. Koppenburg,[7] S. Korpar,[18,12] P. Križan,[17,12] P. Krokovny,[1] C. C. Kuo,[22] A. Kuzmin,[1] Y.-J. Kwon,[47] G. Leder,[10] S. H. Lee,[35] T. Lesiak,[25] J. Li,[34] S.-W. Lin,[24] D. Liventsev,[11] J. MacNaughton,[10] G. Majumder,[38] F. Mandl,[10] T. Matsumoto,[43] A. Matyja,[25] W. Mitaroff,[10] H. Miyata,[27] R. Mizuk,[11] T. Nagamine,[41] Y. Nagasaka,[8] E. Nakano,[28] Z. Natkaniec,[25] S. Nishida,[7] O. Nitoh,[44] S. Ogawa,[39] T. Ohshima,[20] T. Okabe,[20] S. Okuno,[13] S. L. Olsen,[6] W. Ostrowicz,[25] H. Ozaki,[7] P. Pakhlov,[11] H. Palka,[25] C. W. Park,[36] N. Parslow,[37] R. Pestotnik,[12] L. E. Piilonen,[46] A. Poluektov,[1] H. Sagawa,[7] Y. Sakai,[7] N. Sato,[20] T. Schietinger,[16] O. Schneider,[16] J. Schümann,[24] S. Semenov,[11] K. Senyo,[20] R. Seuster,[6] H. Shibuya,[39] B. Shwartz,[1] J. B. Singh,[30] A. Somov,[4] N. Soni,[30] R. Stamen,[7] S. Stanič,[45,*] M. Starič,[12] K. Sumisawa,[29] T. Sumiyoshi,[43] S. Suzuki,[33] S. Y. Suzuki,[7] O. Tajima,[7] F. Takasaki,[7] K. Tamai,[7] N. Tamura,[27] M. Tanaka,[7] Y. Teramoto,[28] X. C. Tian,[31] T. Tsukamoto,[7] S. Uehara,[7] T. Uglov,[11] K. Ueno,[24] S. Uno,[7] K. E. Varvell,[37] S. Villa,[16] C. C. Wang,[24] C. H. Wang,[23] M. Watanabe,[27] B. D. Yabsley,[46] A. Yamaguchi,[41] Y. Yamashita,[26] M. Yamauchi,[7] J. Ying,[31] Y. Yusa,[41] C. C. Zhang,[9] J. Zhang,[7] L. M. Zhang,[34] Z. P. Zhang,[34] V. Zhilich,[1] and D. Žontar[17,12]

(Belle Collaboration)

[1]*Budker Institute of Nuclear Physics, Novosibirsk*
[2]*Chiba University, Chiba*
[3]*Chonnam National University, Kwangju*
[4]*University of Cincinnati, Cincinnati, Ohio 45221*
[5]*Gyeongsang National University, Chinju*
[6]*University of Hawaii, Honolulu, Hawaii 96822*
[7]*High Energy Accelerator Research Organization (KEK), Tsukuba*
[8]*Hiroshima Institute of Technology, Hiroshima*
[9]*Institute of High Energy Physics, Chinese Academy of Sciences, Beijing*
[10]*Institute of High Energy Physics, Vienna*
[11]*Institute for Theoretical and Experimental Physics, Moscow*
[12]*J. Stefan Institute, Ljubljana*
[13]*Kanagawa University, Yokohama*
[14]*Korea University, Seoul*
[15]*Kyungpook National University, Taegu*
[16]*Swiss Federal Institute of Technology of Lausanne, EPFL, Lausanne*
[17]*University of Ljubljana, Ljubljana*
[18]*University of Maribor, Maribor*
[19]*University of Melbourne, Victoria*
[20]*Nagoya University, Nagoya*
[21]*Nara Women's University, Nara*
[22]*National Central University, Chung-li*
[23]*National United University, Miao Li*
[24]*Department of Physics, National Taiwan University, Taipei*
[25]*H. Niewodniczanski Institute of Nuclear Physics, Krakow*
[26]*Nihon Dental College, Niigata*
[27]*Niigata University, Niigata*
[28]*Osaka City University, Osaka*
[29]*Osaka University, Osaka*
[30]*Panjab University, Chandigarh*
[31]*Peking University, Beijing*

[32]*Princeton University, Princeton, New Jersey 08545*
[33]*Saga University, Saga*
[34]*University of Science and Technology of China, Hefei*
[35]*Seoul National University, Seoul*
[36]*Sungkyunkwan University, Suwon*
[37]*University of Sydney, Sydney, New South Wales*
[38]*Tata Institute of Fundamental Research, Bombay*
[39]*Toho University, Funabashi*
[40]*Tohoku Gakuin University, Tagajo*
[41]*Tohoku University, Sendai*
[42]*Department of Physics, University of Tokyo, Tokyo*
[43]*Tokyo Metropolitan University, Tokyo*
[44]*Tokyo University of Agriculture and Technology, Tokyo*
[45]*University of Tsukuba, Tsukuba*
[46]*Virginia Polytechnic Institute and State University, Blacksburg, Virginia 24061*
[47]*Yonsei University, Seoul*
(Received 3 November 2004; published 9 June 2005)

We report on the first observation of $D_1^0(2420) \to D^0\pi^-\pi^+$ and $D_1^+(2420) \to D^+\pi^-\pi^+$ decays (where the contribution from the dominant known $D_1 \to D^*\pi$ decay mode is excluded) in the $B^- \to D_1^0\pi^-$ and $\bar{B}^0 \to D_1^+\pi^-$ decays, respectively. The observation is based on 15.2×10^7 $B\bar{B}$ events collected with the Belle detector at the KEKB collider. We also set 90% confidence level upper limits for the branching fractions of the four following decays: $B^- \to D_1^0\pi^-$, $D_1^0 \to D^{*0}\pi^-\pi^+$, $\bar{B}^0 \to D_1^+\pi^-$, $D_1^+ \to D^{*+}\pi^-\pi^+$, $B^- \to D_2^{*0}(2460)\pi^-$, $D_2^{*0} \to D^{*0}\pi^-\pi^+$, $\bar{B}^0 \to D_2^{*+}(2460)\pi^-$, $D_2^{*+} \to D^{*+}\pi^-\pi^+$.

DOI: 10.1103/PhysRevLett.94.221805 PACS numbers: 13.25.Ft, 12.39.Hg, 13.25.Hw, 14.40.Lb

The ground states of heavy-light quark $c\bar{q}$ system, D and D^* mesons, are well studied. For the D_1 orbital P-wave excitation of the $c\bar{q}$ system only one decay mode $D_1 \to D^*\pi$ is currently known [1]. Measurements of other modes are important to the study of heavy-light quark systems and the production of excited D mesons in B decays. In particular, there is a significant discrepancy in the branching ratio $R = \mathcal{B}(B^- \to D_2^{*0}\pi^-)/\mathcal{B}(B^- \to D_1^0\pi^-)$ between theoretical predictions and current data, if $D_1 \to D^*\pi$ is assumed to saturate the $D_1(2420)$ width.

Calculations based on the heavy quark effective theory (HQET) and the factorization approach [2–4] predict a value $R \sim 0.35$ [4], assuming nonfactorizable corrections are small. Experimental estimates of R are significantly larger. Based on measurements of the ratio $\mathcal{B}(D_2^{*0} \to D^+\pi^-)/\mathcal{B}(D_2^{*0} \to D^{*+}\pi^-)$ [5,6] and a $B^- \to D^{*+}\pi^-\pi^-$ study [7], the CLEO collaboration obtained $R = 1.8 \pm 0.8$. Recently the branching fractions for the decays $B \to D^{**}\pi \to D^{(*)}\pi\pi$ have been measured with better accuracy [8], resulting in $R = 0.77 \pm 0.15$. [We use D^{**} to denote P-wave excitations of the D meson, including $D_1(2420)$ and $D_2^*(2460)$.] These experimental determinations assume that D_1 and D_2^* decays are saturated by the two-body $D\pi$ and $D^{(*)}\pi$ modes, respectively. The existence of $D_{1,2}$ decay channels other than $D_{1,2} \to D^{(*)}\pi$ would modify the R value, possibly lifting the 2.8σ discrepancy between the prediction of Ref. [4] and the experimental results. Measurements of subleading D^{**} decays are also valuable for understanding heavy-light quark systems, given recent unexpected results in the charmed-strange sector [9].

In this Letter we report the first observation of the $D_1^+ \to D^+\pi^-\pi^+$ and $D_1^0 \to D^0\pi^-\pi^+$ decays, and the results of a search for the $D_2^* \to D^{(*)}\pi^+\pi^-$ and $D_1 \to D^*\pi^+\pi^-$ decay modes. The D_1 mesons were reconstructed from the $\bar{B}^0 \to D_1^+\pi^-$ and $B^- \to D_1^0\pi^-$ decays, respectively. The results are based on a sample of $15.2 \times 10^7 B\bar{B}$ pairs produced at the KEKB asymmetric-energy e^+e^- collider [10]. The inclusion of charge conjugate states is implied throughout this Letter.

The Belle detector has been described elsewhere [11]. Charged tracks are selected with a set of requirements based on the average number of hits in the central drift chamber (CDC) and on the distance of the closest approach to the interaction point. Track momentum transverse to the beam axis of at least 0.05 GeV$/c$ is required for all tracks in order to reduce the combinatorial background. For charged particle identification (PID), the combined information from specific ionization in the CDC (dE/dx), time-of-flight scintillation counters, and aerogel Čerenkov counters is used. Charged kaons are selected with PID criteria that have an efficiency of 88%, a pion misidentification probability of 8%, and negligible contamination from protons. All charged tracks with PID responses consistent with a pion hypothesis that are not positively identified as electrons are considered as pion candidates. Photon candidates are selected from calorimeter showers not associated with charged tracks. An energy deposition of at least 30 MeV and a photonlike shape are required for each candidate. Pairs of photons with an invariant mass within 12 MeV$/c^2$ ($\sim 2.5\sigma$) of the π^0 nominal mass [1] are considered as π^0 candidates. These cuts are commonly used in analyses of data collected with the Belle detector to achieve a good signal to background ratio in the selection of these particles.

We reconstruct D^0 (D^+) mesons in the $K^-\pi^+$ ($K^-\pi^+\pi^+$) decay channel and require the invariant mass to be within 15 MeV$/c^2$ ($\sim 3\sigma$) of the D^0 (D^+) mass. The D^{*0} (D^{*+}) mesons are reconstructed in the $D^0\pi^0$ ($D^0\pi^+$) decay mode. The calculated mass difference between D^{*0} (D^{*+}) and D^0 candidates is required to be within 2(1.5) MeV$/c^2$ ($\sim 2.5\sigma$) of the expected value [1]. For $D^* \to D^0\pi$ decays the $D^0 \to K^-\pi^+\pi^+\pi^-$ mode is also included (the same D^* selection criteria were used as above).

We combine $D^{(*)}$ candidates with $\pi^-\pi^-\pi^+$ to form B mesons. Candidate events are identified by their center-of-mass (c.m.) energy difference, $\Delta E = (\Sigma_i E_i) - E_{\rm beam}$, and the beam constrained mass, $M_{\rm bc} = \sqrt{E_{\rm beam}^2 - (\Sigma_i \vec{p}_i)^2}$, where $E_{\rm beam}$ is the beam energy and $\vec{p}_i$ and E_i are the momenta and energies of the decay products of the B meson in the c.m. frame. We define the signal region as $5.273 < M_{\rm bc} < 5.285$ GeV$/c^2$ and $|\Delta E| < 25$ MeV. The sidebands are defined as $5.273 < M_{\rm bc} < 5.285$ GeV$/c^2$ and 25 MeV $< |\Delta E| < 50$ MeV. If there is more than one B candidate (this occurs in 12% of the events), the one with the $D^{(*)}$ mass closest to the nominal value and the best $\pi^-\pi^-\pi^+$ vertex is chosen. We use Monte Carlo (MC) simulation to model the detector response and determine the acceptance [12]. A range of $D_1 \to D\pi\pi$ decay models was used for this simulation (see below), and the resulting variation in efficiency was included in the systematic uncertainty.

Variables that characterize the event topology calculated in the c.m. frame are used to suppress the background from the two-jet-like $e^+e^- \to q\bar{q}$ continuum process. We require $|\cos\theta_{\rm thr}| < 0.80$, where $\theta_{\rm thr}$ is the angle between the thrust axis of the B candidate and that of the rest of the event; this eliminates 77% of the continuum background while retaining 78% of the signal events. We also define a Fisher discriminant, $\mathcal{F}$, which is based on the production angle of the B candidate, the angle of the thrust axis with respect to the beam axis, and nine parameters that characterize the momentum flow in the event [13]. We impose a requirement on $\mathcal{F}$ that rejects 67% of the remaining continuum background and retains 83% of the signal.

To suppress the large contribution from the dominant $D_1 \to D^*\pi \to D\pi\pi$ decay mode, we apply a requirement on the invariant mass of the relevant $D\pi$ combination $|(m_{D\pi} - m_D) - (m_{D^*}^{\rm PDG} - m_D^{\rm PDG})| > 6$ MeV$/c^2$ (10σ) [1].

The ΔE and $M_{D^{(*)}\pi\pi}$ distributions for the selected $B \to D_1\pi$, $D_1 \to D^{(*)}\pi\pi$ candidates are shown in Fig. 1. (To improve the $m_{D^{(*)}\pi\pi}$ mass resolution, we replace it with $m_{D^{**}} = m_{D^{(*)}\pi\pi} - m_{D^{(*)}} + m_{D^{(*)}}^{\rm PDG}$ [1].) To plot the ΔE distributions, we require $M_{\rm bc}$ to lie in the signal region with an additional requirement $|M_{D^{(*)}\pi\pi} - M_{D_1}| < 25$ MeV$/c^2$, where M_{D_1} is the D_1 world average mass value; for the $M_{D^{(*)}\pi\pi}$ distributions we select events from the ΔE signal region. (Although there are two $D\pi^+\pi^-$ combinations, they are kinematically separated in the D_1 mass region.) Clear signals are observed for $B^- \to D_1^0\pi^-$, $D_1^0 \to D^0\pi^-\pi^+$ and $\bar{B}^0 \to D_1^+\pi^-$, $D_1^+ \to D^+\pi^-\pi^+$ decays. For branching fraction calculations we use signal yields determined from the fit to $M_{D\pi\pi}$ distributions as it allows us to directly estimate a possible contribution from the $B \to D_2\pi$, $D_2 \to D\pi\pi$ decay. The signal shape distribution is parametrized by a convolution of a resolution Gaussian ($\sigma = 2.5 \pm 0.6$ MeV$/c^2$, set from MC simula-

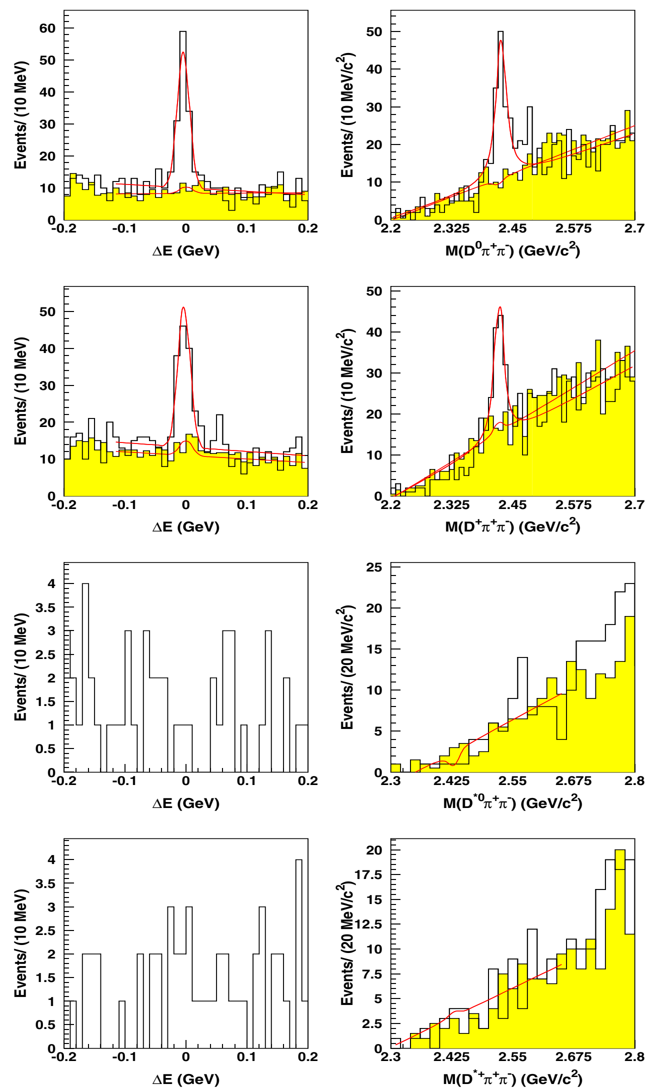

FIG. 1 (color online). ΔE (left) and $M_{D\pi\pi}$ (right) distributions for the $D_1^0 \to D^0\pi^-\pi^+$ (first row), $D_1^+ \to D^+\pi^-\pi^+$ (second row), $D_1^0 \to D^{*0}\pi^-\pi^+$ (third row), $D_1^+ \to D^{*+}\pi^-\pi^+$ (fourth row). Open histograms represent the data from the signal area, solid histograms show the $M_{D\pi\pi}$ (where applicable) and ΔE sidebands, the curves are the fit results—for the signal area and sidebands.

tion) with a signal Breit-Wigner function; the background is represented by a linear function. (The D^{*+} width in data was used to validate the MC estimate of detector resolution.) The D_1 mass and width determined from the fit are $M_{D_1^0} = 2426 \pm 3 \pm 1\ \mathrm{MeV}/c^2$ (statistical and systematic error, respectively), $\Gamma_{D_1^0} = 24 \pm 7 \pm 8\ \mathrm{MeV}/c^2$ for D_1^0 and $M_{D_1^+} = 2421 \pm 2 \pm 1\ \mathrm{MeV}/c^2$, $\Gamma_{D_1^+} = 21 \pm 5 \pm 8\ \mathrm{MeV}/c^2$ for D_1^+; these are consistent with the world average values [1]. The signal yields are given in Table I: the first and second errors on the branching fraction products are statistical and systematic, and the third is a model uncertainty due to other possible sources of D_1 production, and contributions from D_2^*, discussed below. For the $B \to D_1\pi \to D^*\pi^-\pi^-\pi^+$ decay channels, we do not observe statistically significant signals and thus determine 90% C.L. upper limits [14] for their branching fractions. In the fit to the $M_{D^*\pi\pi}$ distribution, we fix the D_1 mass and width at their world average values. The statistical significance of signals quoted in Table I is defined as $\sqrt{-2\ln(L_0/L_{\max})}$, where $L_{\max}$ and L_0 denote the maximum likelihood with the nominal signal yield and with the signal yield fixed at zero, respectively.

To account for contamination from other possible D_1 production mechanisms (such as $e^+e^- \to c\bar{c}$ continuum production or semileptonic $B \to D_1 l\bar{\nu}$ decays), we fit the $M_{D\pi\pi}$ distribution for events in the ΔE sidebands. In this fit, we fix the D_1 mass and width at their world average values. The fits give -6 ± 8 events for the D_1^0 and 10 ± 11 events for the D_1^+. The resulting uncertainties in the D_1 yields are $^{+0}_{-10}\%$ for the D_1^0 and $+0 - 22\%$ for the $D_1^{\pm}$.

The $B \to D_2^*(2460)\pi$, $D_2^* \to D\pi^+\pi^-$ decay may also contribute to the $B \to D\pi^-\pi^-\pi^+$ final state. To check for a possible effect, we perform a simultaneous fit to the $M(D_1^0\pi^+\pi^-)$ and $M(D_1^+\pi^+\pi^-)$ distributions, where we assume isospin invariance and require the ratio $N(D_2^*)/N(D_1)$ to be the same for both charge combinations. The fit finds the ratio $N(D_2^*)/N(D_1) = 0.33 \pm 0.14$ and signal yields of $N(D_1^0) = 120 \pm 17$, $N(D_1^+) = 107 \pm 16$. While an excess can be seen near the $D_2^*(2460)$ mass in $D_1^0 \to D^0\pi^-\pi^+$, there is no evidence of an enhancement in the $D_1^+ \to D^+\pi^-\pi^+$ mode (see Fig. 1); we set a 90% C.L. upper limit on the D_2^* contribution of $\mathcal{B}(B \to D_2^*\pi^-) \times \mathcal{B}(D_2^* \to D\pi^+\pi^-) < 0.51\mathcal{B}(B \to D_1\pi^-) \times \mathcal{B}(D_1 \to D\pi^+\pi^-)$ [15], and determine the $D_1(2420)$ yield from the fit without $D_2^*(2460)$. Fixing the $\frac{D_2^*}{D_1}$ ratio to 0.47 results in a change of -21% in the D_1 yield: this is combined in quadrature with the uncertainty from other possible D_1 sources, to obtain the "model" uncertainty in Table I.

The signal yields extracted from the ΔE distributions are used only to verify that there is no significant contribution to the signal from the non-D_1 peak region. The ΔE signal shape is parametrized by a Gaussian with parameters determined from signal MC simulation. The ΔE background shape is described by a linear function. We restrict the fit to the range $-0.1 < \Delta E < 0.2$ GeV to avoid contributions from other B decays, where an additional pion is not reconstructed. Signal yields obtained from the fits to ΔE distributions are 106 ± 12 for $D^0\pi^+\pi^-$ and 96 ± 13 for $D^+\pi^+\pi^-$, while the corresponding reconstruction efficiencies are 10.8% and 7.6%, respectively. Thus, the event yields obtained from the two methods are consistent.

In order to determine the $D_1 \to D\pi\pi$ partial width, an analysis of final states with neutral pions is required. With only the $D_1 \to D\pi^+\pi^-$ branching fraction measurement, an analysis of the decay dynamics could also be useful to determine the total $D_1 \to D\pi\pi$ width. As the limited statistics do not allow us to perform a full amplitude analysis, we consider the one-dimensional projections of several variables: $M_{D\pi}$, $M_{\pi^+\pi^-}$, $\cos\Theta(\pi_B^-\pi_{D^{**}}^-)$, $\cos\Theta(\pi_B^-\pi_{D^{**}}^+)$, and $\cos\Theta(\pi_B^- D)$ (where all angles are calculated in the D^{**} rest frame). Although these variables are not independent, they highlight each model's features. For instance, the helicity angle distributions differentiate between the $D_1 \to D(\pi\pi)$ and $D_1 \to (D\pi)\pi$ models. We select events from the B signal region with the additional requirement $|M(D\pi\pi) - M_{D_1}| < 25\ \mathrm{MeV}/c^2$. Decays through the following quasi-two-body intermediate states are considered: $D_1 \to D\rho^0 \to D\pi^+\pi^-$, $D_1 \to D_0^*(2308)\pi \to D\pi\pi$, and $D_1 \to Df_0(600) \to D\pi^+\pi^-$ [we set $M_{f_0} = 0.8\ \mathrm{GeV}/c^2$ and $\Gamma_{f_0} = 0.8\ \mathrm{GeV}/c^2$; the $D_0^*(2308)$ parameters are taken from Ref. [8]]. We use the simplest nontrivial Lorentz-invariant expressions for the corresponding matrix elements in MC simulation [16]. We fit the experimental data with different models. For each variable we plot two distributions: one from the signal region and the other from the ΔE sideband. We perform a simultaneous fit to these distributions, assuming a Poisson-like profile in each bin whose mean is the sum of the

TABLE I. Number of events, efficiencies and branching fraction products of $B \to D^{**}\pi$, $D^{**} \to D^{(*)}\pi^+\pi^-$ decays.

Mode	N_{sig}	$\varepsilon(10^{-2})$	$\mathcal{B}(B \to D_{1(2)}^{(*)}\pi) \times \mathcal{B}(D_{1(2)}^{(*)} \to D^{(*)}\pi)(10^{-4})$	Significance
$B^- \to D_1^0\pi^-$, $D_1^0 \to D^0\pi^-\pi^+$	151 ± 24	14.1	$(1.85 \pm 0.29 \pm 0.35^{+0.0}_{-0.43})$	8.7σ
$\bar{B}^0 \to D_1^+\pi^-$, $D_1^+ \to D^+\pi^-\pi^+$	124 ± 20	9.9	$(0.89 \pm 0.15 \pm 0.17^{+0.0}_{-0.27})$	10σ
$B^- \to D_1^0\pi^-$, $D_1^0 \to D^{*0}\pi^+\pi^-$	<1.2	2.2	<0.06	⋯
$\bar{B}^0 \to D_1^+\pi^-$, $D_1^+ \to D^{*+}\pi^+\pi^-$	<12.0	3.4	<0.33	⋯
$B^- \to D_2^{*0}\pi^-$, $D_2^{*0} \to D^{*0}\pi^+\pi^-$	<4.4	2.2	<0.22	⋯
$\bar{B}^0 \to D_2^{*+}\pi^-$, $D_2^{*+} \to D^{*+}\pi^+\pi^-$	<9.0	3.4	<0.24	⋯

background and signal (for a given model) in the signal region or the background only in the sideband. The obtained differences of likelihood values for all variables are listed in Table II. Figure 2 shows the $M_{\pi^+\pi^-}$ and $\cos\Theta(\pi_B^- D)$ distributions along with expectations based on different $D_1 \to D\pi^+\pi^-$ decay models [17]. Although the $D_1 \to D_0^*\pi$ decay mechanism describes the data best, some contribution from other mechanisms cannot be excluded completely.

It is interesting to examine the dependence of the R value on the decay mechanism. The expression for R can be written as $s_1 \times \mathcal{B}(B^- \to D_2^{*0}\pi^-, D_2^{*0} \to D^{*+}\pi^-)/(s_1 \times \mathcal{B}(B^- \to D_1^0\pi^-, D_1^0 \to D^{*+}\pi^-) + s_2 \times \mathcal{B}(B^- \to D_1^0\pi^-, D_1^0 \to D^0\pi^+\pi^-))$ where s_i is a scale factor that recovers the full width from the single decay channel. (These scale factors include the branching fractions of all relevant D^{**}, D^*, and D subdecays; the s_i factors are calculated from Clebsch-Gordan coefficients for each of the three models, without accounting for any possible interference effects.) Following the procedure used in Ref. [8] and fixing s_1 at $3/2$, we can calculate s_2 factors for different models: $s_2(D^{**0} \to D_0^{*+}\pi^-) = 9/4$ (disregarding possible interference effects in $D_1^0 \to D^+\pi^-\pi^0$ decays), $s_2(D^{**0} \to D^0\rho) = 3$, $s_2(D^{**0} \to D^0 f_0) = 3/2$. Using the branching fractions measured in Ref. [8] and here, the central value for R depends on the decay model in the following way: 0.50 for $D\rho$, 0.60 for Df_0, and 0.54 for $D_0^*\pi$.

The following sources of systematic errors are considered: tracking efficiency (8% overall, integrated over particle momenta), kaon identification efficiency (2% overall), π^0 reconstruction efficiency (8%), D branching fraction uncertainties (2%–7%), MC statistics (2%), model uncertainty in MC efficiency (10%), uncertainty caused by variation of cuts (5%), background shape uncertainty (10%). The uncertainty in the tracking efficiency is estimated using partially reconstructed $D^{*+} \to D^0[K_S^0\pi^+\pi^-]\pi^+$ decays. The kaon identification uncertainty is determined from $D^{*+} \to D^0[K^-\pi^+]\pi^+$ decays. The π^0 reconstruction uncertainty is obtained using D^0 decays to $K^-\pi^+$ and $K^-\pi^+\pi^0$. To determine the systematic uncertainty in the signal yield extraction, we use different parametrizations for the background events. The overall systematic uncertainty is 19% for $B \to D\pi\pi\pi$ and 21% for $B \to D^*\pi\pi\pi$. We assume equal production rates for B^+B^- and $B^0\bar{B}^0$ pairs and do not include the corresponding uncertainty in the total systematic error.

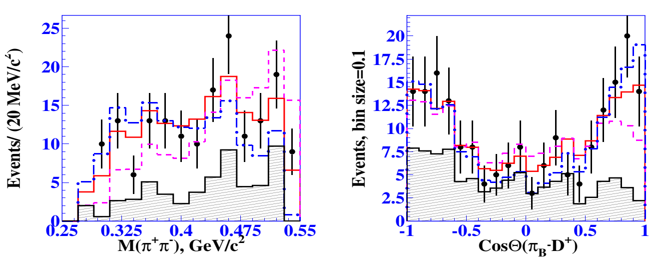

FIG. 2 (color online). $M_{\pi^+\pi^-}$ (left) and $\cos\Theta(\pi_B^- D)$ (right) distributions for the $D_1^0 \to D^0\pi^-\pi^+$ and $D_1^+ \to D^+\pi^-\pi^+$, respectively. Points with error bars represent the experimental data, solid line—$D^{*0}\pi$, dashed—$D\rho$, chain—Df_0 models with the expected background added. The hatched histogram corresponds to expected background (from ΔE sidebands).

The $B^- \to D^0\pi^+\pi^-\pi^-$ final state also includes the $D^{*+}\pi^-\pi^-$ intermediate state with $D^{*+} \to D^0\pi^+$. We reverse the D^* veto requirement to select $D^{*+}\pi^+\pi^-$ events and measure the branching ratio $\mathcal{B}(B^- \to D^{*+}\pi^-\pi^-) = (1.27 \pm 0.07) \times 10^{-4}$ (based on a sample of $85 \times 10^6 B\bar{B}$ events), which agrees well with the value of $\mathcal{B}(B^- \to D^{*+}\pi^-\pi^-) = (1.25 \pm 0.07) \times 10^{-4}$ measured earlier [8].

In summary, we report the first observation of $D_1(2420) \to D\pi^+\pi^-$ decays (with the dominant $D_1 \to D^*\pi$ contribution excluded). The measured branching ratios of the $B^- \to D_1^0\pi^-$, $D_1^0 \to D^0\pi^-\pi^+$ and $\bar{B}^0 \to D_1^+\pi^-$, $D_1^+ \to D^+\pi^-\pi^+$ decays with the corresponding statistical significances and systematic uncertainties are presented in Table I. We find the upper limit for the possible D_2^* contribution to these results: $\mathcal{B}(B \to D_2^*\pi^-) \times \mathcal{B}(D_2^* \to D\pi^+\pi^-) < 0.51\mathcal{B}(B \to D_1\pi^-) \times \mathcal{B}(D_1 \to D\pi^+\pi^-)$. No statistically significant signal has been observed for the $D^{**} \to D^*\pi^+\pi^-$ decays. The corresponding 90% C.L. upper limits are listed in Table I. Analysis of the $D_1 \to D\pi^+\pi^-$ dynamics shows that the decay model $D_1 \to D_0^*\pi$ gives the best description of the data. The $R = \mathcal{B}(B^- \to D_2^{*0}\pi^-)/\mathcal{B}(B^- \to D_1^0\pi^-)$ value calculated assuming $D_1 \to D_0^*\pi$ dominates is 0.54 ± 0.18; this is $\sim 2\sigma$ lower than the previously published one and is consistent with the expectation for R from HQET and factorization [4].

We thank the KEKB group for the excellent operation of the accelerator, the KEK cryogenics group for the efficient operation of the solenoid, and the KEK computer group and the NII for valuable computing and Super-SINET network support. We acknowledge support from MEXT and JSPS (Japan); ARC and DEST (Australia); NSFC (Contract No. 10175071, China); DST (India); the BK21 program of MOEHRD and the CHEP SRC program of

TABLE II. The likelihood values for the $D_1 \to D\rho(L_{D\rho})$ and $D_1 \to Df_0(L_{Df_0})D_1 \to D\pi\pi$ decay models in Goodness-of-fit tests compared to the $D_1 \to D_0^*\pi(L_{D_0^*\pi})$ model.

Distribution	$(-2\ln L_{D\rho}/L_{D_0^*\pi})^{1/2}$	$(-2\ln L_{Df_0}/L_{D_0^*\pi})^{1/2}$
	D^0, D^+	D^0, D^+
$M_{D\pi}$	2.5, 2.7	1.9, 2.9
$M_{\pi^+\pi^-}$	3.4, 1.6	5.2, 4.7
$\cos\Theta(\pi_B^-\pi_{D^{**}}^+)$	1.6, 2.5	-2.0^{a}, 3.4
$\cos\Theta(\pi_B^-\pi_{D^{**}}^-)$	2.5, 3.0	4.0, 2.9
$\cos\Theta(\pi_B^- D)$	2.0, 0.5	3.2, 4.0

[a]In this case $L_{Df_0} < L_{D_0^*\pi}$.

KOSEF (Korea); KBN (Contract No. 2P03B 01324, Poland); MIST (Russia); MESS (Slovenia); SNSF (Switzerland); NSC and MOE (Taiwan); and DOE (USA).

*On leave from Nova Gorica Polytechnic, Nova Gorica.

[1] S. Eidelman *et al.*, Phys. Lett. B **592**, 1 (2004).

[2] A. Ali and C. Greub, Phys. Rev. D **57**, 2996 (1998).

[3] A. K. Leibovich, Z. Ligeti, I. W. Stewart, and M. B. Wise, Phys. Rev. D **57**, 308 (1998).

[4] M. Neubert, Phys. Lett. B **418**, 173 (1998).

[5] P. Avery *et al.* (CLEO Collaboration), Phys. Lett. B **331**, 236 (1994); **342**, 453(E) (1995).

[6] H. Albrecht *et al.* (ARGUS Collaboration), Phys. Lett. B **232**, 398 (1989).

[7] J. Gronberg *et al.* (CLEO Collaboration), CLEO-CONF 96-25, contribution to the 28th International Conference on High Energy Physics, Warsaw, Poland, 1996 (unpublished)..

[8] K. Abe *et al.* (Belle Collaboration), Phys. Rev. D **69**, 112002 (2004).

[9] B. Aubert *et al.* (*BABAR* Collaboration), Phys. Rev. Lett. **90**, 242001 (2003); D. Besson *et al.* (CLEO Collaboration), Phys. Rev. D **68**, 032002 (2003); P. Krokovny *et al.* (Belle Collaboration), Phys. Rev. Lett. **91**, 262002 (2003); Y. Mikami *et al.* (Belle Collaboration), Phys. Rev. Lett. **92**, 012002 (2004).

[10] S. Kurokawa and E. Kikutani, Nucl. Instrum. Methods Phys. Res., Sect. A **499**, 1 (2003).

[11] A. Abashian *et al.* (Belle Collaboration), Nucl. Instrum. Methods Phys. Res., Sect. A **479**, 117 (2002).

[12] R. Brun *et al.*, GEANT 3.21, CERN Report No. DD/EE/84-1.

[13] D. M. Asner *et al.* (CLEO Collaboration), Phys. Rev. D **53**, 1039 (1996).

[14] G. J. Feldman and R. D. Cousins, Phys. Rev. D **57**, 3873 (1998).

[15] We use the mean $+1.28\sigma$ construction to set the limit. As most of the systematic uncertainties cancel in the ratio of the branching fractions, the systematic uncertainty is negligible.

[16] We use the following expressions for matrix elements for the $D_1 \to D\pi\pi$ decay: $F^{\nu\eta}(B^0, \pi_B^+)F_{\mu\nu}(\bar{D}_0^*, \pi_{D_1^-}^-)P(D_1^-)_\eta P(D_1^-)^\mu$, $F^{\phi\eta}(B^0, \pi_B^+)F_{\mu\phi}(f^0, D^-)P(D_1^-)_\eta P(D_1^-)^\mu$, $F^{\nu\eta}(B^0, \pi_B^+)F_{\nu\mu}(\rho^0, \pi_\rho^+ - \pi_\rho^-)P(D_1^-)_\eta P(D_1^-)^\mu$, where the following notation is used: $F^{\mu\nu}(A, B) = P_A^\mu P_B^\nu - P_A^\nu P_B^\mu$, $P(B - C) = P(B) - P(C)$, and P stands for a 4-momentum.

[17] In the case of the Df_0 model the key $\cos\Theta(\pi_B^- D)$ distribution is practically independent of the f_0 mass and width.